Hindawi
Advances in Civil Engineering
Volume 2020, Article ID 8848924, 7 pages
https://doi.org/10.1155/2020/8848924

Research Article

Karst Water Pressure's Varying Rule and Its Response to Overlying Strata Movement in Coal Mine

Jian Hao, Hua Bian, Anfa Chen, Jiahui Lin, and Dongjing Xu

State Key Laboratory of Mining Disaster Prevention and Control, Shandong University of Science and Technology, Qingdao 266590, China

Correspondence should be addressed to Hua Bian; bh199512@163.com

Received 23 April 2020; Revised 14 July 2020; Accepted 25 July 2020; Published 7 August 2020

Academic Editor: Richeng Liu

Karst water is widespread throughout China and is heavily influenced by complex geological conditions, and floor inrush of karst waters associated with coal seams is the second most common coal mine disaster in China. Due to the limitation of precision and cost of geophysical exploration technology, the volume and pressure of karst water are challenging to measure, especially during the mining process. Therefore, predicting karst pressure's response to mining is critical for determining the mechanism of water inrush. Here, closed karst water pressure (CKWP) response to mining was studied in an innovative physical simulation experiment. In the simulation experiment, a capsule and a pipe were designed to reflect CKWP and the water level. In the experiment, the vertical stress and karst water level were monitored throughout the process of an advancing coal panel. Monitoring results show that the range of the abutment pressure was about 40 cm, and the peak coefficient value was about 2. When the working face is far away from the water capsule, the stress and water column near the water capsule have no obvious change. With the working face 10 cm from the water capsule, the stress and water column height increased significantly. When the working face was right above the water capsule, the stress and water column rose sharply and reached the maximum value. When the working face advanced beyond the water capsule, the stress and water column height declined. Through establishing a structural mechanics model, the karst water system underneath the working face is assumed to be a hydraulic press. Accordingly, the compressed area was assumed to be a piston. The karst water pressure increases sharply, while the piston is compressed, increasing water inrush risk. This discovery may help determine the water inrush mechanism from a novel point of view.

1. Introduction

China contains some of the most abundant limestone karsts throughout the world [1, 2]. These karsts typically occur in the Ordovician limestones, with the accumulated thickness in some areas with tens of kilometers [3–5]. The limestone distribution is shown in Figure 1. Influenced by complex hydrogeological conditions, mine water inrush accidents frequently occur in the process of coal mining in China in these heavily karst regions [6–8]. In recent years, water inflow and inrush have also frequently occurred during the construction of coal mine in the Southwestern, China. According to incomplete statistics, there have been more than 3,000 mine water inrush accidents, among which floor water inrush accidents caused by Ordovician limestone aquifers account for about 30% of these accidents. Many of these floor inrush accidents often lead to flooding of the entire mine and loss of life and property [9–11].

In 1964, during the "Hydrogeology Battle" organized by the Ministry of Coal Industry of China in the Jiaozuo mining area, the water inrush coefficient method was put forward to establish a method to predict water inrush during mining. It is based on a comprehensive analysis of existing water inrush accidents. The water inrush coefficient (T) refers to the water pressure that can be borne by an aquifer having a unit thickness. It is expressed using the following equation [12–14]:

$$T = \frac{P}{M}, \tag{1}$$

where P is the water pressure of the aquifer and M is the thickness of the aquiclude of the floor.

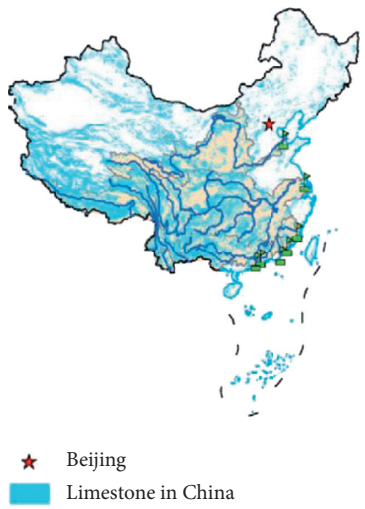

Figure 1: Distribution map of limestone in China.

Additionally, the water inrush from the coal seam floor is the result of many factors, including water pressure, ore pressure, the thickness of the aquiclude, the thickness of key strata, and the distribution of faults and folds [15, 16].

According to theory and engineering [17–22], the karst water pressure is the power source for these floor water inrush disasters. Understanding the variations and mechanisms of karst water pressure is vital for controlling floor water inrush disasters.

In the past, the water level would be estimated by the difference in height between target points to the water level. This viewpoint provides essential support for the prevention and control of mine water inrush disasters. However, in underground mining, the working face is removable, so the overlying strata structure continuously varies during mining, as well as the strata structure itself and mining stress are continuously readjusting to compensate for the removal of the working face [23–25]. Overall, strata movement and mining stress may have some influences on karst water pressure underneath the floor. Because water is incompressible from a macro perspective, it typically does not respond to pressure from strata movement, especially for closed karst systems. However, few studies have focused on karst water pressure's response to strata movement caused by mining in the subsurface.

In the present study, closed karst water pressure (CKWP) response to mining is presented and analyzed by a physical similarity experiment. A conceptual structural mechanical model was established to verify the karst water pressure varying rule in the whole process of coal panel advancing. Experimental results helped to determine the mechanisms of floor water inrush and can provide specific guidance for the prevention of mine water inrush accidents.

2. Materials and Methods

2.1. Similarity Principle and Similarity Coefficient. In order to study closed karst pressure's characteristics and its response to mining, a similar material experiment was carried out. A similar material experiment is an effective method to discuss and understand ground pressure systems in scientific research, especially in the coal mining field. It uses an experimental model to simulate the engineering site according to a scaled-down version at corresponding proportions. The model is made from similar materials according to similarity theory, which has similar mechanical characteristics as each stratum, and stress and deformation are monitored during the excavation process [25]. Here the geometric similarity coefficient between the model and the prototype was 1/70. According to the similarity principle, the similarity coefficients to be satisfied are as follows [26, 27].

2.1.1. Geometric Similarity Coefficient (α_L). The coefficient of geometric similarity is as follows:

$$\alpha_L = \frac{X_m}{X_h} = \frac{Z_m}{Z_h} = \frac{Y_m}{Y_h} = \frac{1}{70}. \quad (2)$$

2.1.2. Bulk Density Similarity Coefficient (α_τ). According to the rock bulk density of the prototype, the bulk density of the experimental model is

$$\alpha_\tau = \frac{\gamma_m}{\gamma_h} = \frac{1}{90}. \quad (3)$$

2.1.3. Time Similarity Coefficient (α_t). Because the acceleration of gravity of the prototype and the experimental model are equal, the time similarity coefficient is

$$\alpha_t = \sqrt{\alpha_L} = \frac{1}{8}. \quad (4)$$

2.1.4. Stress Similarity Coefficient (α_σ). According to similarity theory and $\alpha_t = \sqrt{\alpha_L}$, the stress similarity constant is calculated by substituting the bulk density similarity coefficient and geometric similarity coefficient into the following formula:

$$\alpha_\sigma = \alpha_\gamma \cdot \alpha_1 = \frac{1}{90} \times \frac{1}{8} = \frac{1}{720}. \quad (5)$$

2.2. Engineering Background and Similar Material Experiment Model. Based on the geological conditions of the #5 coal seam in a coal mine as the engineering background, the immediate roof of the #5 coal face is primarily sandstone, with an average thickness of 7 m. The main roof is principally fine-grained sandstone, with an average thickness of 5.6 m. The immediate floor is also sandstone, with an average thickness of 12.6 m. In this similar simulation test, similar materials composed of sand, lime, gypsum, and water were mixed with particular proportions according to the lithology of each section of strata. According to the determined similarity constant, the proportional parameters of each layer in the similar simulation test are listed in Table 1.

The similar materials experiments were conducted based on the geological conditions of the mine in order to analyze karst water pressures response to movement and stress transfer in the overlying strata. The general framework is shown in Figure 2. The similar materials simulation model had a length, width, and height of 120 cm, 40 cm, and 70 cm, respectively. The working face advancing distance was 80 cm, and each mining step was 10 cm. 20 cm boundary coal pillars were set at both ends of the model to eliminate the boundary effect. A water capsule filled with water was embedded in the floor under the coal seam in advance to simulate a closed karst water system, as shown in Figure 3. A communicating tube, connected to the water capsule, was installed to observe the water level and indicate karst water pressure, as shown in Figure 4. Stress sensors were installed under the coal seam every 10 cm to monitor the vertical stress on the floor, as shown in Figure 5. The final model is shown in Figure 6. Throughout the experiment, a camera was used to record the movement of the overlying strata, and stress sensors recorded the vertical stress fluctuations in the floor in real time. In order to observe the water level clearly, water in the water capsule and the communicating tube was colored by black pigment.

3. Experimental Results

3.1. Movement of the Roof Rock Stratum. The whole process of the overlying strata movement is shown in Figure 7. As can be seen from Figure 7, when the working face advanced to 35 cm, the immediate roof composed sandstone with a thickness of 7 m collapsed. When the working face advanced to 54 cm, the immediate roof started to collapse periodically, the main roof started to bend, and several strata started to separate. Finally, the main roof further broke from low to high. The range of strata movement was approximately an arch shape. The final development height of the fracture zone was 33.6 cm, about ten times the lowest height.

3.2. Varying Rule of Floor Stress and Karst Water Pressure. During the advancement of the working face, the overlying strata moved, as shown in Figure 8. Furthermore, the stress surrounding the working face was redistributed. With the advancement of the working face, the stress sensor installed in the floor monitored vertical stress in real time, and the water level in the communicating tube was observed in real time. The initial height of CKWP is shown in Figure 8. In order to understand the karst water pressure response to vertical stress, we focused on the vertical stress above the water capsule on the floor, as shown in Figure 9. The horizontal axis indicates the distance from the working face to the monitoring point, and the vertical axis indicates the vertical stress on the floor and the water level height. The variations in the vertical stress and water level are described according to the monitoring results. It can be seen from Figure 9 that the range of influence of the abutment pressure was about 40 cm (28 m), and the stress peak coefficient value was about 2. When the working face was at 40 cm, the vertical stress started to increase. As the coal wall approached the monitoring point above the water capsule, the vertical stress gradually increased. When the coal wall reached the monitoring point, the vertical stress peaked. As the coal wall advanced over the monitoring point above the water capsule, the vertical stress decreased to some extent.

Furthermore, the water level rose although with a time lag compared to the increasing vertical stress. The initial water level height of 27 cm scarcely changes in the initial stage of advancement. When the coal wall was 10 cm to the water capsule, the water level began to increase. With the advancement of the coal wall, the water level continued to rise. When the coal wall advanced above the water capsule, the peak water level is 44 cm. After the coal wall advanced beyond the water capsule, the water level dropped to 26 cm.

It can be seen from Figure 9 that when the working face is far from the water capsule, there are no obvious changes in the stress near the water capsule and water column. With the working face becoming closer to the water capsule, the stress and water column height significantly increased. When the working face further advanced near the water capsule, the stress and water column rose sharply and reached their maximum values. When the working face advanced beyond the water capsule, the stress and water column height declined. Overall, the advancement of the working face appears to only affect the water level and stress locally.

4. Discussion

As shown in Figure 9, the CKWP would increase during the advancement of working face. This indicates that the karst water pressure has some response to movements of the overburden caused by mining. The reason should be considered from a novel visual angle. Further discussion is necessary to determine some interesting phenomena neglected in previous studies.

The area of the immediate roof overhang gradually increased with the advancement of the working face and finally collapsed when the overhanging length of roof was beyond 40 cm. At this point, the upper strata started to bend and separate. The strata move gradually from bottom to top with the advancement of the working face. According to the classical ground pressure theory, the overburden can be divided into the collapsing zone, fracture zone, and bending zone from bottom to top.

During the advancement of the working face, the vertical stress at the monitoring point above the karst cave did not change initially. When the working face advanced to 40 cm, the weight of the overburden transferred to the coal wall in front of the working face, and the vertical stress started to increase. It continued to gradually increase with the advancement of the working face until the coal panel passed beyond the monitoring point. Notably, the CKWP increased throughout the process of the vertical stress increasing to 60 kPa.

In order to analyze this phenomenon, we established a conceptual structural mechanics model, as shown in Figure 10. The top part of the model demonstrates the structural mechanical model of the stope, and the bottom section of the model is the closed karst system. A high-stress zone

Table 1: Material ratio of each rock stratum.

Lithology	Depth of stratum (m)	Proportion (sand : gypsum : lime)	Thickness (cm)	Stratified weight (kg)	Stratified number	Sand (kg)	Gypsum (kg)	Lime (kg)	Water (kg)
Sandstone	6.3	7 : 0.3 : 0.7	3	38.59	3	33.77	1.45	3.38	3.22
Siltstone	4.9	7 : 0.2 : 0.8	4	29.56	2	25.87	2.96	0.74	2.46
Fine sandstone	5.6	7 : 0.8 : 0.2	4	30.72	2	26.88	1.15	2.69	2.56
Sandstone	7	7 : 0.3 : 0.7	3	33.98	3	29.73	1.27	2.97	2.83
#5 coal seam	2.1	6 : 0.3 : 0.7	3	37.44	1	32.09	1.6	3.74	3.12
Sandstone	12.6	7 : 0.3 : 0.7	3	34.42	6	30.99	1.33	3.1	2.87

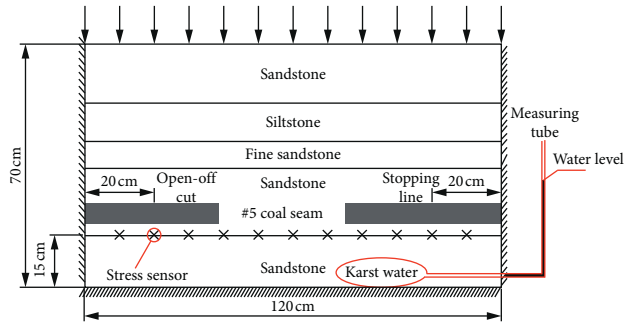

Figure 2: Overall structure of simulation model.

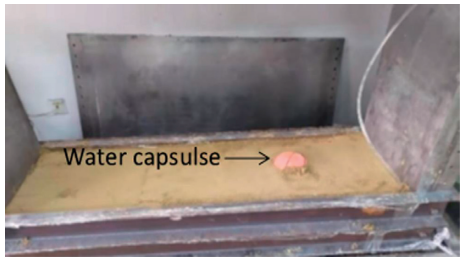

Figure 3: Location of water capsule installed in model.

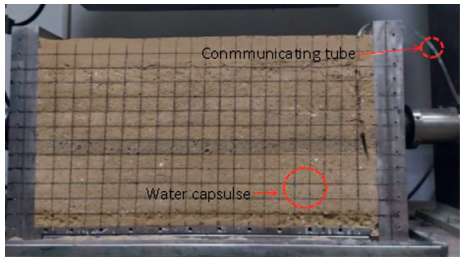

Figure 4: Sketch map of communicating tube.

Figure 5: Sketch map of stress sensor in floor.

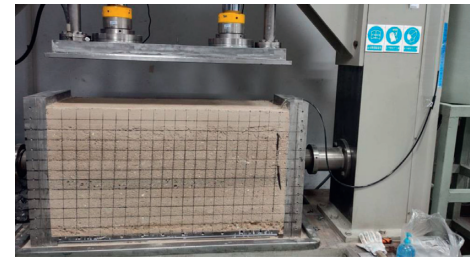

Figure 6: Real product of simulation model.

gradually forms around the working face due to movement of the overburden strata, and the floor under high-stress area is compressed. Because the compressibility of water is negligible, the pressure is transferred to the karst cavity wall without a reduction in closed karst system. In this situation, the closed karst system under the coal panel can be regarded as a hydraulic system, as shown in Figure 11. The floor strata in the high-stress zone are compressed, similar to a piston by the upper strata. If the pressure is higher than a certain level, compression deformation occurs, and the pressure would then transfer to the surrounding karst cavity wall by the incompressible water.

When the working face advances beyond the closed karst system, the upper strata in the monitoring area collapse and

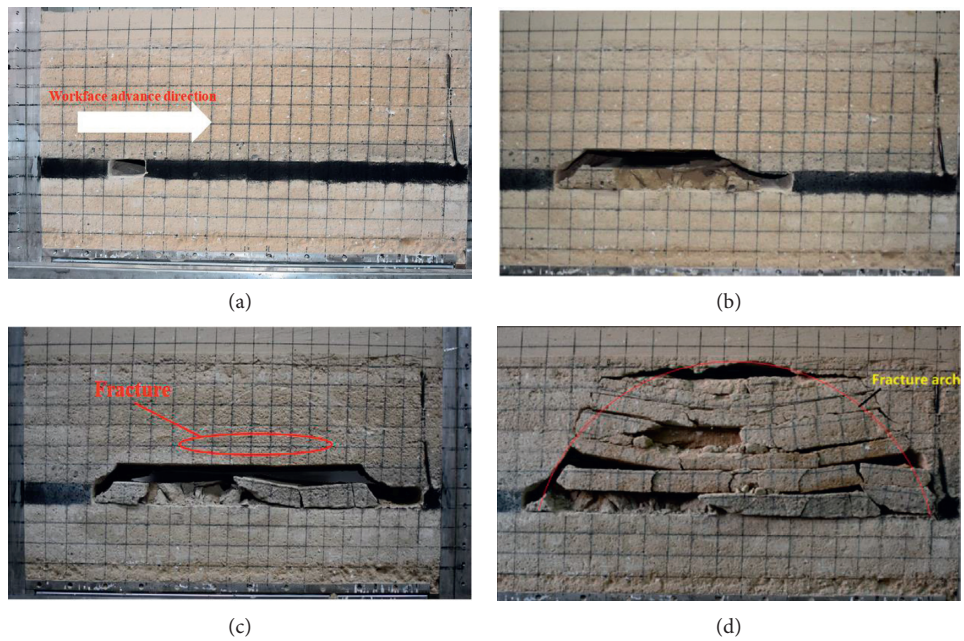

Figure 7: The process of strata movement with working face advancing: (a) no coal mining; (b) immediate roof first collapse; (c) separation of main roof; (d) fracture arch formation.

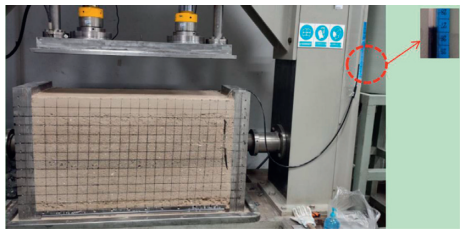

Figure 8: Initial height of CKWP.

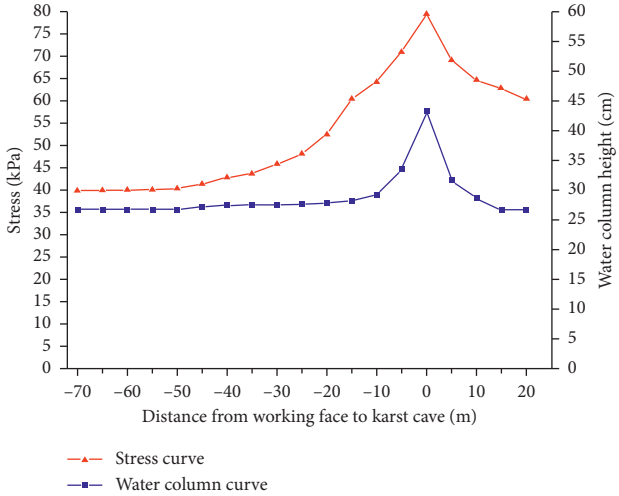

Figure 9: Varying curve of vertical stress and water level height.

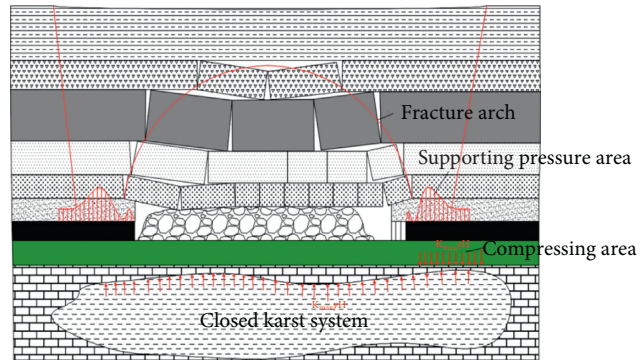

Figure 10: Structural mechanical model of the closed karst system with stope.

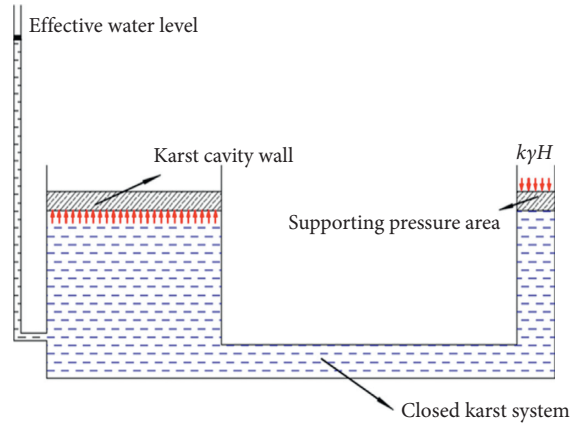

Figure 11: Mechanical model of hydraulic system.

compress the floor strata. The stress of the floor rock and the water pressure of the karst system decreases. It is not difficult to infer that advancing the working face as quickly as possible, to put the karst system under the goaf without extended periods of high stress is an effective method to control floor water inrush disasters.

5. Conclusions

In this paper, the closed karst water pressure response to mining was presented and analyzed by conducting a similarity experiment. The experimental study was designed to determine variations in stress and water levels in a CKWP caused by mining. A conceptual structural mechanical model was created to describe the karst water pressure response to mining. From the model and experimental study above, several interesting conclusions can be drawn.

Karst water pressure appears to have some relationship caused by mining with the overlying strata. Floor karst water and its pressure should be considered with moving strata caused by mining as a whole system. It is not static and unchanging but might be influenced by the overburden movement throughout the advancement process of the working face.

According to experimental results, the pressure of the floor water might increase sharply, when disturbed by mining supporting pressure, especially when the karst water system is closed. While the floor rock mass above the karst water system is compressed, the floor rock mass would move like a piston, which would then cause deformation of the karst cavity. At this point, the CKWP would rise, and the risk of a floor water inrush disaster would increase.

Indeed, not all types of karst water systems have an apparent response to mining stress caused by the overlying strata movement, as sealing capacity of the key to keep the mine from communicating with the karst. The pressure within the karst system would respond to the increased stress directly above the aquifer, as the karst would have a better sealing capacity. The mining stress would also cause microdeformation of the floor.

We found that this discovery might be helpful in determining floor water inrush mechanisms. Furthermore, it provides an innovative angle for methods to control water inrush in mining.

Data Availability

The data used to support the findings of this study are available from the corresponding author upon request.

Conflicts of Interest

The authors declare that they have no conflicts of interest.

Acknowledgments

The research presented in this paper has been supported jointly by the National Natural Science Foundation of China (Grant nos. 5180 4180 and 51574055), Key Research Plan of Shandong Province (Grant no. 2018GSF116007), Natural Science Foundation of Shandong Province (Grant no. ZR2017BEE033), Postdoctoral Innovation Foundation of Shandong Province (201703076), and "Top Disciplines" Special Project of Mining and Safety Engineering College (1SY04602).

References

[1] Y. Zhao, F. Wang, C. Li, Y. Cao, and H. Tian, "Study of the corrosion characteristics of tunnel fissures in a karst area in Southwest China," *Geofluids*, vol. 2018, Article ID 6234932, 19 pages, 2018.

[2] Q. Wu, L. T. Xing, and C. H. Ye, Y. Z. Liu, The influences of coal mining on the large karst springs in North China," *Environmental Earth Sciences*, vol. 64, no. 6, pp. 1513–1523, 2009.

[3] J. Pu, M. Cao, Y. Zhang, D. Yuan, and H. Zhao, "Hydrochemical indications of human impact on karst groundwater in a subtropical karst area, Chongqing, China," *Environmental Earth Sciences*, vol. 72, no. 5, pp. 1683–1695, 2014.

[4] V. Festa, A. Fiore, M. Parise, and A. Siniscalchi, "Sinkhole evolution in the apulian karst of southern Italy: a case study, with some considerations on sinkhole hazards," *Journal of Cave and Karst Studies*, vol. 74, no. 2, pp. 137–147, 2012.

[5] Z. Liu, C. Groves, D. Yuan, and J. Meiman, "South China karst aquifer storm-scale hydrochemistry," *Ground Water*, vol. 42, no. 4, pp. 491–499, 2004.

[6] Q.-L. Cui, H.-N. Wu, S.-L. Shen, Y.-S. Xu, and G.-L. Ye, "Chinese karst geology and measures to prevent geohazards during shield tunnelling in karst region with caves," *Natural Hazards*, vol. 77, no. 1, pp. 129–152, 2015.

[7] H. Jian, Y. Shi, J. Lin et al., "The effects of backfill mining on strata movement rule and water inrush: a case study," *Processes*, vol. 7, no. 2, 2018.

[8] R. K. Tiwary, "Environmental impact of coal mining on water regime and its management," *Water, Air, and Soil Pollution*, vol. 132, no. 1-2, pp. 185–199, 2001.

[9] X. Sun, H. Fu, G. Kou, L. Liu, P. Li, and L. Miao, "Mechanism of water hazard caused by the secondary separation in the overburden stratum of the fully mechanized coal face," *Journal of Mining and Safety Engineering*, vol. 34, no. 4, pp. 678–683, 2017.

[10] V. Palchik, "Localization of mining-induced horizontal fractures along rock layer interfaces in overburden: field measurements and prediction," *Environmental Geology*, vol. 48, no. 1, pp. 68–80, 2005.

[11] Z. Meng, G. Li, and X. Xie, "A geological assessment method of floor water inrush risk and its application," *Engineering Geology*, vol. 143-144, pp. 51–60, 2012.

[12] C. S. Hao, R. Zhao, and M. Cai, "Safety evaluation of 11# coal seam pressure mining in Sangshuping Coal Mine," *Coal Technology*, vol. 4, 2018.

[13] W. Qiao, W. P. Li, and C. X. Zhao, "Water inrush coefficient-unit inflow method for water inrush evaluation of coal mine floor," *Chinese Journal of Rock Mechanics and Engineering*, vol. 28, no. 12, pp. 002466–002474, 2009.

[14] B. Y. Li and Z. G. Jing, "Preliminary study on safe mining of coal seams threatened by Ordovician limestone confined water," *Journal of Shandong University of Science and Technology*, vol. 1, pp. 67–84, 1980.

[15] A. C. Ekeleme and J. C. Agunwamba, "Experimental determination of dispersion coefficient in soil," *Emerging Science Journal*, vol. 2, no. 4, pp. 213–218, 2018.

[16] A. Tahershamsi, A. Feizi, and S. Molaei, "Modeling groundwater surface by MODFLOW math code and geostatistical method," *Civil Engineering Journal*, vol. 4, no. 4, pp. 812–827, 2018.

[17] L. Shi and Z. Song, "Evaluation for the water inrush possibility in the deep mining of Feicheng coal field (in Chinese)," *Journal of China Coal Society*, vol. 25, no. 3, pp. 273–277, 2000.

[18] F. Gong and J. Lu, "Recognition method of mine water inrush sources based on the principal element analysis and distance discrimination analysis," *Journal of Mining & Safety Engineering*, vol. 31, no. 2, pp. 236–242, 2014.

[19] J. Lu, X. Li, F. Gong, X. Wang, and J. Liu, "Recognizing of mine water inrush sources based on principal components analysis and Fisher discrimination analysis method," *China Safety Science Journal*, vol. 22, no. 7, pp. 109–115, 2012.

[20] C. Simsek, A. Elci, O. Gunduz, and B. Erdogan, "Hydrogeological and hydrogeochemical characterization of a karstic mountain region," *Environmental Geology*, vol. 54, no. 2, pp. 291–308, 2008.

[21] P. N. Gamaletsos, A. Godelitsas, T. Kasama et al., "Nanomineralogy and -geochemistry of high-grade diasporic karst-type bauxite from Parnassos-Ghiona mines, Greece," *Ore Geology Reviews*, vol. 84, pp. 228–244, 2017.

[22] T. Robineau, A. Tognelli, P. Goblet, F. Renard, and Schaper, "A double medium approach to simulate groundwater level variations in a fissured karst aquifer," *Journal of Hydrology*, vol. 565, pp. 861–875, 2018.

[23] W. Qiao, W. Li, and X. Li, "Mechanism of "hydrostatic water-inrush" and countermeasures for water inrush in roof bed separation of a mining face," *Journal of Mining & Safety Engineering,* vol. 28, no. 1, pp. 96–104, 2011.

[24] W. Qiao, Y. Huang, Z. Yuan, and W. Guo, "Formation and prevention of water inrush from roof bed separation with full-mechanized caving mining of ultra thick coal seam Chin," *Journal of Rock Mechanics and Geotechnical Engineering*, vol. 33, no. 10, pp. 2076–2084, 2014.

[25] X. Li, *Study on the Inrush Mechanism of the Water in Bed Separation Due to Repeated Coal Mining under Hard Rock*, China University of Mining and Technology, Xuzhou, China, 2011.

[26] W. Liu, "Experimental and numerical study of rock stratum movement characteristics in longwall mining," *Shock and Vibration*, vol. 2019, Article ID 5041536, 15 pages, 2019.

[27] X. Zhang, H. Yu, J. Dong et al., "A physical and numerical model-based research on the subsidence features of overlying strata caused by coal mining in Henan, China," *Environmental Earth Sciences*, vol. 7620 pages, 2017.